

The effect of multivalent cation dopants on lithium manganese spinel cathodes

A. de Kock, E. Ferg^{*}, R.J. Gummow

Division of Materials Science and Technology, CSIR, P.O. Box 395, Pretoria, 0001, South Africa

Received 6 September 1996; revised 24 April 1997

Abstract

The cycling stability of 4 V $\text{Li}_x\text{Mn}_2\text{O}_4$ electrodes in lithium, flooded electrolyte glass cells has been improved by the addition of multivalent cation dopants (Mg^{2+} , Zn^{2+} and Al^{3+}). Optimal dopant levels to achieve maximum capacity and the greatest stability with repeated cycling have been determined. The effect of doping the oxygen-rich spinel $\text{Li}_2\text{Mn}_4\text{O}_9$ was also determined and shown to make no significant improvement in the life cycle stability in the 3 V region. © 1998 Elsevier Science S.A.

Keywords: Lithium manganese; Spinel; Cation doping

1. Introduction

The $\text{Li}_x\text{Mn}_2\text{O}_4$ spinel ($0 \leq x \leq 1$) is a well known cathode for 4 V lithium batteries [1–5]. However $\text{Li}/\text{Li}_x\text{Mn}_2\text{O}_4$ cells lose capacity gradually when cycled in the 4 V range [6]. This capacity loss has been attributed to several factors [7]: (i) a gradual dissolution of manganese in the electrolyte solution; (ii) loss of cathode integrity on deep discharge due to the large volume changes which occur in the spinel lattice when $x \geq 1$ in $\text{Li}_x\text{Mn}_2\text{O}_4$. These volume changes are as a result of the Jahn–Teller distortion of Mn^{3+} cations which occurs when the average manganese valency is approximately 3.5 [3]; and (iii) an instability of the electrolyte at the high voltages reached on charge.

Recent work has shown that, when the Mn^{3+} -ion concentration in the spinel material is reduced by the addition of appropriate dopants (Li^+ , Mg^{2+} or Zn^{2+}), improved cycling stability in the 4 V range could be achieved [7]. Guohua et al. [8] demonstrated the improved cycling stability of LiMn_2O_4 doped with Co, Cr and Ni. The improvement in stability was explained as being a result of:

1. suppression of the Jahn–Teller effect on deep discharge,

2. the presence of residual lithium in fully charged electrodes,
3. stabilisation of the octahedral sites in the spinel skeleton structure, and
4. a reduction in the volume changes during cycling.

The synthesis of lithium manganese oxide cathodes at lower temperatures, approximately 400–450°C, has been reported [2,9,10]. These compounds, for example $\text{Li}_2\text{Mn}_4\text{O}_9$ and $\text{Li}_4\text{Mn}_5\text{O}_{12}$, can discharge at a voltage of approximately 3 V vs. lithium and exhibit improved cycling performance in the voltage range when compared with $\text{Li}_x\text{Mn}_2\text{O}_4$ ($1 \leq x \leq 2$). The improved cycling stability has been attributed, at least in part, to the delay in the onset of the Jahn–Teller distortion in these compounds until late in the discharge cycle [4]. Nevertheless these compounds also lose capacity slowly when cycled repeatedly. Studies on doped CDMO (composite electrode containing a lithiated $\gamma\text{-MnO}_2$ and a spinel phase) with Bi and V oxides showed an improved cycling ability in the 3 V region when compared with undoped CDMO [11]. The question then arises whether $\text{Li}_2\text{Mn}_4\text{O}_9$ might also be stabilised by the addition of dopants in an analogous manner.

In this study, the stabilising effects of the multivalent cations Mg^{2+} , Zn^{2+} and Al^{3+} in defect spinel systems with general formula $\text{LiMn}_{2-d}\text{M}_{d/b}\text{O}_{4+\delta}$ where d is the dopant content ($0 < d \leq 0.15$), b is the valency of M and δ ($0 \leq \delta \leq 0.5$), the excess oxygen, have been investigated

^{*} Corresponding author.

further. The aim of this investigation is to determine optimised spinel cathode compositions that can be used in lithium cells.

2. Experimental

$\text{LiMn}_{2-d}\text{M}_{d/b}\text{O}_{4+\delta}$ spinels with $\text{M} = \text{Mg}^{2+}, \text{Zn}^{2+}$ and Al^{3+} , $0 < d \leq 0.15$, $b = 2$ or 3 and $\delta = 0$ were synthesised by reaction of the required stoichiometric amounts of $\text{LiOH} \cdot \text{H}_2\text{O}$, MnO_2 and either $\text{Mg}(\text{NO}_3)_2 \cdot 6\text{H}_2\text{O}$, $\text{Zn}(\text{NO}_3)_2 \cdot 2\text{H}_2\text{O}$ or $\text{Al}(\text{NO}_3)_3 \cdot 9\text{H}_2\text{O}$, respectively in air. The powders were thoroughly mixed, prior to firing, by ball-milling in hexane. Samples were heat treated at 450°C for 48 h and thereafter at 650°C for 48–96 h.

The oxygen-rich spinels $\text{LiMn}_{2-d}\text{M}_{d/b}\text{O}_{4+\delta}$ were doped with Mg^{2+} ($d = 0.05$ and 0.02); Zn^{2+} ($d = 0.05$, 0.03 and 0.02) and Al^{3+} ($d = 0.05$ and 0.03) respectively. They were synthesised by firing in the temperature range 300 – 400°C . Selected samples were also synthesised at 450°C with Mg^{2+} ($d = 0.10$), Zn^{2+} ($d = 0.03$) and Al^{3+} ($d = 0.05$), respectively.

Powder X-ray diffraction data were collected on an automated Rigaku diffractometer with $\text{CuK}\alpha$ radiation, monochromated with a graphite single crystal. The lattice constants of starting materials and of oxidised cathodes were obtained by iterative least-squares refinements against a silicon standard. The oxidised cathodes were obtained by removing the cathodes from electrochemical cells after equilibration following the first charge cycle to the upper voltage limit.

Electrochemical studies were performed using a prismatic lithium cell with a flooded-electrolyte system assem-

bled under Argon gas at room temperature. The cathode material consisted of 80% by mass of the spinel and 20% by mass of the 1:2 mixture of acetylene black and teflon (TAB). The cathode material was pressed onto a 10 mm diameter stainless steel mesh current collector. The anode consisted of lithium foil (Lithco) pressed onto a stainless steel mesh. The electrolyte used was a 1 M LiClO_4 solution in anhydrous propylene carbonate (Aldrich). The anode and cathode were separated by a microporous polypropylene separator (Celgard 3401). The cells in the 4 V region were cycled between 4.4 V and 3.5 V with a charge current of 0.2 mA and a discharge current of 0.4 mA. The cells containing the oxygen-rich cathodes were cycled between 3.9 V and 2.0 V or 2.2 V with the same currents as for the 4 V system.

For comparative purposes, electrochemical cells were made with standard laboratory prepared $\text{Li}_2\text{Mn}_4\text{O}_9$ [9], LiMn_2O_4 [12] and a purchased LiMn_2O_4 standard (JEC-3) [13].

3. Results and discussion

Table 1 summarises the data for the doped spinels studied in the 4 V region with their respective experimental lattice constants and their theoretical capacities based on the mass of the fully oxidised material. The Zn doped materials for $d = 0.1$ and 0.15 were not synthesised because their theoretical capacities showed them to be irrelevant for any practical application. All samples can be referred to the general formula $\text{LiMn}_{2-d}\text{M}_{d/b}\text{O}_{4+\delta}$ where M is either Mg^{2+} , Zn^{2+} or Al^{3+} , $0 < d \leq 0.15$, b , the valency of the M cation, is 2 or 3 and $\delta = 0$; that is the

Table 1
Properties of $\text{Li}/\text{LiMn}_{2-d}\text{M}_{d/b}\text{O}_{4+\delta}$ spinel phases synthesized at high temperatures

Stoichiometry of spinel phases	d	Experimental lattice constant (\AA)	Theoretical Mn oxidation state	Fully oxidised composition	Theoretical capacity ^a (mA h/g)	Lattice constant of oxidised spinel electrode ^b (\AA)
LiMn_2O_4	0	8.2314(2)	3.5	Mn_2O_4	153.65	8.0608(3)
$\text{LiMn}_{1.97}\text{Al}_{0.01}\text{O}_4$	0.03	8.2173(2)	3.5381	$\text{Li}_{0.09}\text{Mn}_{1.97}\text{Al}_{0.01}\text{O}_4$	140.44	8.0800(4)
$\text{LiMn}_{1.95}\text{Al}_{0.018}\text{O}_4$	0.05	8.2190(2)	3.5641	$\text{Li}_{0.15}\text{Mn}_{1.95}\text{Al}_{0.018}\text{O}_4$	132.03	8.0740(3)
$\text{LiMn}_{1.90}\text{Al}_{0.033}\text{O}_4$	0.1	8.2138(2)	3.6316	$\text{Li}_{0.3}\text{Mn}_{1.90}\text{Al}_{0.033}\text{O}_4$	109.14	8.0765(3)
$\text{LiMn}_{1.85}\text{Al}_{0.05}\text{O}_4$	0.15	8.2062(2)	3.7027	$\text{Li}_{0.45}\text{Mn}_{1.85}\text{Al}_{0.05}\text{O}_4$	86.326	8.0817(3)
$\text{LiMn}_{1.98}\text{Mg}_{0.01}\text{O}_4$	0.02	8.2185(2)	3.5253	$\text{Li}_{0.06}\text{Mn}_{1.98}\text{Mg}_{0.01}\text{O}_4$	144.80	8.0694(3)
$\text{LiMn}_{1.95}\text{Mg}_{0.025}\text{O}_4$	0.05	8.2123(2)	3.5641	$\text{Li}_{0.15}\text{Mn}_{1.95}\text{Mg}_{0.025}\text{O}_4$	131.44	8.0590(3)
$\text{LiMn}_{1.90}\text{Mg}_{0.05}\text{O}_4$	0.10	8.1989(2)	3.6316	$\text{Li}_{0.3}\text{Mn}_{1.90}\text{Mg}_{0.05}\text{O}_4$	108.93	8.0788(3)
$\text{LiMn}_{1.98}\text{Zn}_{0.01}\text{O}_4$	0.02	8.2185(2)	3.5253	$\text{Li}_{0.06}\text{Mn}_{1.98}\text{Zn}_{0.01}\text{O}_4$	144.46	8.0637(3)
$\text{LiMn}_{1.97}\text{Zn}_{0.015}\text{O}_4$	0.03	8.2175(2)	3.5381	$\text{Li}_{0.09}\text{Mn}_{1.97}\text{Zn}_{0.015}\text{O}_4$	139.86	8.0582(3)
$\text{LiMn}_{1.95}\text{Zn}_{0.025}\text{O}_4$	0.05	8.2177(2)	3.5641	$\text{Li}_{0.15}\text{Mn}_{1.95}\text{Zn}_{0.025}\text{O}_4$	130.66	8.0606(3)
$\text{LiMn}_{1.90}\text{Zn}_{0.05}\text{O}_4^c$	0.1		3.6316	$\text{Li}_{0.3}\text{Mn}_{1.90}\text{Zn}_{0.05}\text{O}_4^c$	107.65	
$\text{LiMn}_{1.85}\text{Zn}_{0.075}\text{O}_4^c$	0.15		3.7027	$\text{Li}_{0.45}\text{Mn}_{1.85}\text{Zn}_{0.075}\text{O}_4^c$	84.62	

$0 < d < 0.15$; $b =$ valency of M; $\delta = 0$.

^aTheoretical capacity, based on the mass of the fully oxidised composition, when discharged to the composition, $\text{LiMn}_{2-d}\text{M}_{d/b}\text{O}_4$.

^bLattice constant of the oxidised electrode determined at the end of the first charge cycle to 4.4 V.

^cCompounds were not prepared and tested.

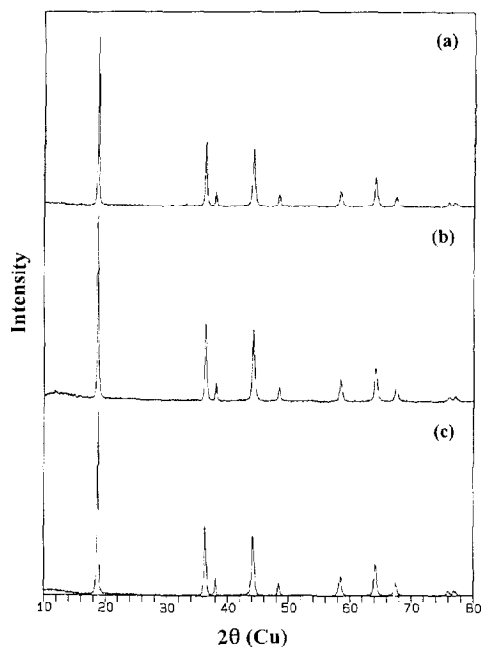


Fig. 1. X-ray diffraction patterns of doped spinel samples synthesised at high temperatures. (a) $\text{LiMn}_{2-d}\text{Al}_{d/3}\text{O}_4$; (b) $\text{LiMn}_{2-d}\text{Mg}_{d/2}\text{O}_4$, (c) $\text{LiMn}_{2-d}\text{Zn}_{d/2}\text{O}_4$ where $d = 0.05$.

samples are all defect spinels [7]. This distinguishes the materials from other doped stoichiometric spinels studied by previous investigators [8,14].

The powder X-ray diffraction patterns of the samples synthesised for this study could be indexed to the spinel space group ($Fd3m$) [12]. All doped materials studied had similar diffraction patterns and Fig. 1 shows some typical examples. A slight decrease in initial lattice constant with increased dopant concentration was found when compared with the lattice constant of the stoichiometric spinel LiMn_2O_4 (Table 1). This is in agreement with the trend observed for lithium-doped spinels, i.e., $M = \text{Li}$ [7,15]. The lattice constant variations are very similar for the different dopants.

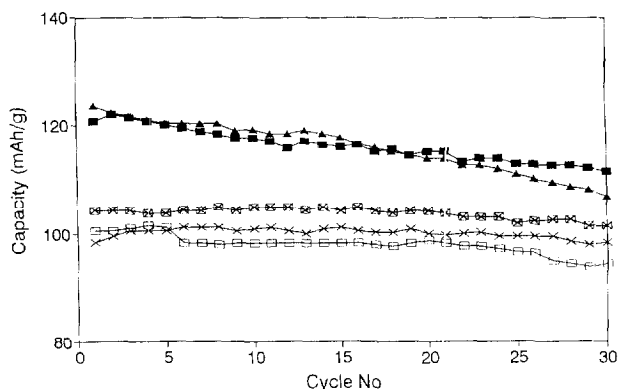


Fig. 2. Discharge capacity vs. cycle number for $\text{Li}/\text{LiMn}_{2-d}\text{Zn}_{d/2}\text{O}_4$ cells in the 4 V region where; ▲ = JEC3; ■ = LiMn_2O_4 ; ⊠, $d = 0.05$; □, $d = 0.03$. and ×, $d = 0.02$.

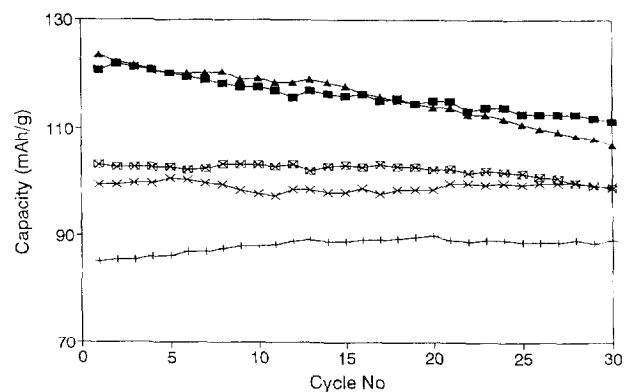


Fig. 3. Discharge capacity vs. cycle number for $\text{Li}/\text{LiMn}_{2-d}\text{Mg}_{d/2}\text{O}_4$ cells in the 4 V region where; ▲ = JEC3; ■ = LiMn_2O_4 ; +, $d = 0.10$; ⊠, $d = 0.05$ and ×, $d = 0.02$.

The lattice constants of oxidised electrodes, removed from an electrochemical cell after the first charge cycle, were also determined. The lattice constants of the oxidised samples do not vary systematically with the dopant concentration. However, due to the lower initial lattice constants observed for doped samples, the lattice constant variations on cycling doped samples are less than those for standard LiMn_2O_4 .

Discharge capacity vs. the number of cycles for $\text{Li}/\text{LiMn}_{2-d}\text{M}_{d/b}\text{O}_{4+\delta}$ cells with $M = \text{Zn}^{2+}$, Mg^{2+} or Al^{3+} at various dopant levels and $\delta = 0$ are shown in Figs. 2–4, respectively. Fig. 5 shows some typical examples of the galvanostatic cycling data for the doped materials studied where $d = 0.05$. The cells containing doped cathodes were on average 80% efficient when compared to their expected theoretical capacities (Table 1). The trends for the Al^{3+} doped materials in Fig. 4 showed that lower capacities were obtained with an increase in d . This is consistent with the theoretical values in Table 1 where a decrease in capacity is expected with an increase in dopant level. The trends for the Zn^{2+} and Mg^{2+} doped materials in Figs. 2 and 3, respectively were inconstant with theoret-

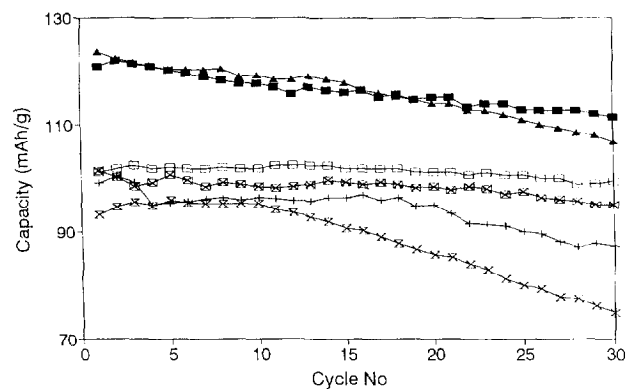


Fig. 4. Discharge capacity vs. cycle number for $\text{Li}/\text{LiMn}_{2-d}\text{Al}_{d/3}\text{O}_4$ cells in the 4 V region where; ▲ = JEC3; ■ = LiMn_2O_4 ; ⊠, $d = 0.15$; +, $d = 0.10$; ⊠, $d = 0.05$ and □, $d = 0.03$.

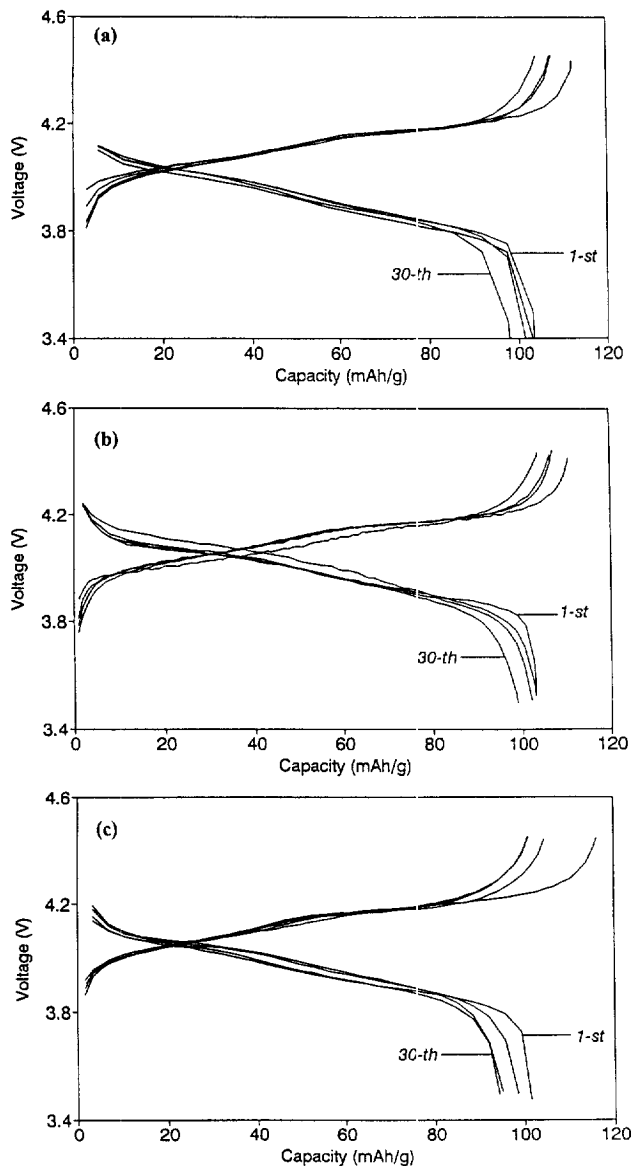


Fig. 5. Typical example of galvanostatic cycling data for Li/LiMn_{2-d}M_{d/2}O₄ cells, (a) M = Zn, (b) M = Mg and (c) M = Al where $d = 0.05$.

ical values as shown in Table 1. The results showed that the higher doped ($d = 0.05$) performed slightly better than the lower ones ($d = 0.02$ and 0.03). This means that for the Zn²⁺ and Mg²⁺ dopants, the optimum dopant level for capacity and life cycle ability would be approximately $d = 0.05$. No reason could be given for such a trend.

After 30 cycles standard Li/Li_xMn₂O₄ cells have lost typically 10–13% of their initial capacity. In general, the lithium manganese cathode materials with Mg, Zn or Al dopants showed improved cycle ability with little loss in capacity after 30 cycles except in the case of high levels of Al doping ($d = 0.10$ and 0.15). However, the improved stability is at the expense of capacity. This can be understood from Table 1 which shows that as the dopant levels

increase, the theoretical capacities of the cathodes decrease. The standard Li/LiMn₂O₄ cell loses capacity largely because the LiMn₂O₄ cathode becomes tetragonally distorted at the end of discharge in the 4.0 V region, that is, when the average manganese oxidation state is 3.5 (Table 1). The doped LiMn_{2-d}M_{d/b}O₄ spinels have an average manganese oxidation state greater than 3.5 with the specific value dependent on the doping level. These doped spinels can therefore tolerate discharge onto the 3 V plateau while still retaining cubic symmetry [7]. This could account for their improved cycling stability when compared to the undoped material.

The lattice constant variations on cycling the doped spinels are also smaller than those for LiMn₂O₄. This results in a more stable lattice and improved capacity retention. This finding is in agreement with the results of Guohua et al. [8] who reported a reduction in volume changes on cycling in the doped spinels LiM_yMn_{2-y}O₄ for M = Co, Cr and Ni where $y = 1/12, 1/9, 1/6$ and $1/3$.

The powder X-ray diffraction patterns of the doped oxygen-rich spinels with general formula LiMn_{2-d}M_{d/b}O_{4+δ} where $d = 0.05$ and $δ ≈ 0.5$ made at 400°C are shown in Fig. 6. The samples are all two-phase with broad peaks that are characteristic of a predominant spinel phase and a minor lithiated $γ$ -MnO₂ phase similar to those described by Thackeray et al. [16]. Samples synthesised at 450°C showed a reduction in the lithiated $γ$ -MnO₂ phase and consisted essentially of a single phase doped spinel (Fig. 7).

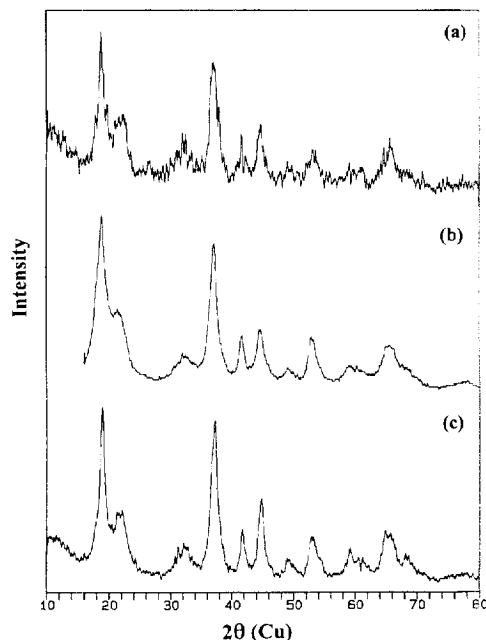


Fig. 6. X-ray diffraction patterns of doped oxygen-rich spinel LiMn_{2-d}M_{d/b}O_{4+δ} compounds synthesized at 400°C. (a) M = Al, (b) M = Mg, and (c) M = Zn where $d = 0.05$ and $δ ≈ 0.5$.

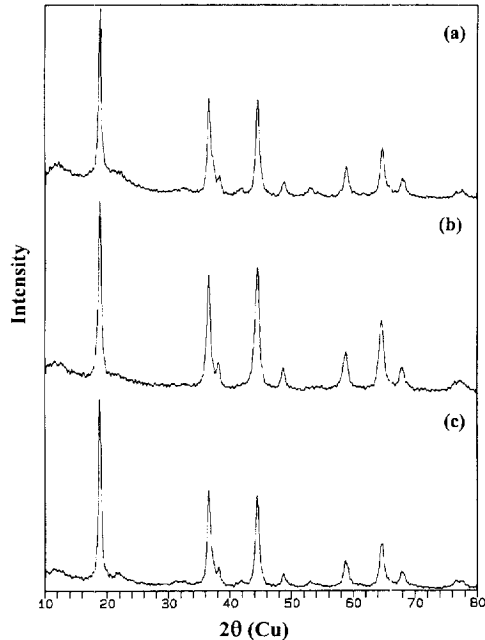


Fig. 7. X-ray diffraction patterns of doped oxygen-rich spinel $\text{LiMn}_{2-d}\text{M}_{d/b}\text{O}_{4+\delta}$ compounds synthesised at 450°C . (a) $\text{M} = \text{Mg}$, $d = 0.10$; (b) $\text{M} = \text{Al}$, $d = 0.05$ and (c) $\text{M} = \text{Zn}$, $d = 0.03$ where $\delta \approx 0.5$.

In general, the cycling performance in the 3 V region of the doped oxygen-rich spinels made at 400°C are not significantly better than the standard $\text{Li}_2\text{Mn}_4\text{O}_9$. An in-

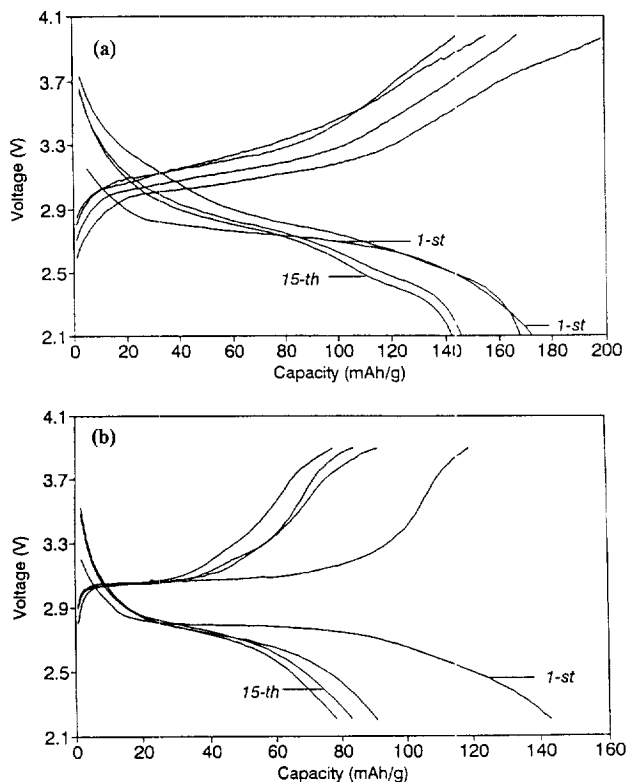


Fig. 8. Typical example of galvanostatic cycling data for a lithium cell with oxygen-rich doped spinel cathodes $\text{LiMn}_{2-c}\text{Zn}_{d/2}\text{O}_{4+\delta}$ synthesized (a) at 400°C where $d = 0.05$ and (b) at 450°C where $d = 0.03$ and $\delta \approx 0.5$.

crease in the discharge capacities of the doped oxygen-rich spinels after the first charge cycle was observed when compared to the standard $\text{Li}_2\text{Mn}_4\text{O}_9$. However, this only persisted for the first few cycles where a s-shaped discharge curve typical of a multi-phase product was observed. The discharge capacities of the doped samples made at 450°C showed no improvement in cycle life and capacity retention when compared to the standard $\text{Li}_2\text{Mn}_4\text{O}_9$. The typical s-shaped discharge curves were not observed for the first few cycles as in the previous samples, showing the characteristics of a more single-phase material. The doped oxygen rich $\text{LiMn}_{2-d}\text{M}_{d/b}\text{O}_{4+\delta}$ synthesized at the higher temperature would lose more oxygen, which would drive the composition towards a doped $\text{LiMn}_{2-d}\text{M}_{d/b}\text{O}_4$ spinel. Fig. 8a,b shows typical galvanostatic cycling data for doped $\text{Li}_2\text{Mn}_4\text{O}_9$ made at the two temperatures respectively.

4. Conclusion

The doped spinels studied in the 4 V region showed that the dopant level of $d = 0.05$ optimise both stability and capacity in Mg-, Zn- and Al-doped spinel electrodes. Lower dopant levels still improve the stability compared to standard LiMn_2O_4 but give capacities very similar or even slightly inferior to those of cathodes with $d = 0.05$. In the case of Al-doped spinels, the initial capacity is not maintained after about 10 cycles when the dopant level $d > 0.05$.

The oxygen-rich doped spinels studied in the 3 V region showed no improvement in capacity when compared to the standard $\text{Li}_2\text{Mn}_4\text{O}_9$. Whereas, the studies done by Li et al. [11] showed an improvement in cycle ability of CDMO doped with Bi and V.

References

- [1] M.M. Thackeray, J.B. Goodenough, U.S. Patent 4,507,371 (1985).
- [2] M.H. Rossouw, A. de Kock, L.A. de Picciotto, M.M. Thackeray, W.I.F. David, R.M. Ibberson, Mater. Res. Bull. 25 (1990) 173.
- [3] M.M. Thackeray, W.I.F. David, P.G. Bruce, J.B. Goodenough, Mater. Res. Bull. 18 (1983) 461.
- [4] M.M. Thackeray, A. de Kock, M.H. Rossouw, D.C. Liles, R. Bittihn, D. Hoge, J. Electrochem. Soc. 139 (1992) 363.
- [5] Y. Xia, H. Takeshige, H. Noguchi, M. Yoshio, J. Power Sources 56 (1995) 61.
- [6] A. Momchilov, V. Manev, A. Nassalevska, A. Kozawa, J. Power Sources 41 (1993) 305.
- [7] R.J. Gummow, A. de Kock, M.M. Thackeray, Solid State Ionics 69 (1994) 59.
- [8] L. Guohua, H. Ikuta, T. Uchia, W. Wakihara, J. Electrochem. Soc. 143 (1) (1996) 178.
- [9] A. de Kock, M.H. Rossouw, L.A. de Picciotto, M.M. Thackeray, Mater. Res. Bull. 25 (1990) 657.

- [10] T. Nohma, T. Saito, N. Furukawa, H. Ikeda, *J. Power Sources* 26 (1989) 389.
- [11] Li, Z Shi, C. Yang, H Yang, *J. Power Sources* 44–45 (1995) 533.
- [12] M.M. Thackeray, L.A. de Picciotto, A. de Kock, P.J. Johnson, V.A. Nicholas, K.T. Adendorff, *J. Power Sources* 21 (1986) 1.
- [13] V. Manev, *JEC-3 Batt. Newsletter* 3 (1994) 33.
- [14] J.M. Tarascon, E. Wang, F.K. Shokoobi, W.R. McKinnon, S. Colson, *J. Electrochem. Soc.* 138 (1991) 1859.
- [15] Y. Gao, J.R. Dahn, *J. Electrochem. Soc.* 143 (1996) 100.
- [16] M.M. Thackeray, M.H. Rossouw, A. de Kock, A.P. de la Harpe, R.J. Gummow, K. Pearce, D.C. Liles, *J. Power Sources* 43–44 (1993) 289.